ELSEVIER

Biochimica et Biophysica Acta 1511 (2001) 224–235

BIOCHIMICA ET BIOPHYSICA ACTA

BBA

www.bba-direct.com

Conformation and orientation of the gene 9 minor coat protein of bacteriophage M13 in phospholipid bilayers

M. Chantal Houbiers [a,*], Cor J.A.M. Wolfs [a], Ruud B. Spruijt [a], Yves J.M. Bollen [a], Marcus A. Hemminga [a], Erik Goormaghtigh [b]

[a] *Department of Biomolecular Sciences, Laboratory of Molecular Physics, Wageningen University and Research Center, Dreijenlaan 3, 6703 HA Wageningen, The Netherlands*

[b] *Laboratoire de Chimie Physique des Macromolécules aux Interfaces, CP206/2, Université Libre de Bruxelles, Campus Plaine, B-1050 Brussels, Belgium*

Received 4 September 2000; received in revised form 2 November 2000; accepted 8 November 2000

Abstract

The membrane-bound state of the gene 9 minor coat protein of bacteriophage M13 was studied in model membrane systems, which varied in lipid head group and lipid acyl chain composition. By using FTIR spectroscopy and subsequent band analysis a quantitative analysis of the secondary structure of the protein was obtained. The secondary structure of the gene 9 protein predominantly consists of α-helical (67%) and turn (33%) structures. The turn structure is likely to be located C-terminally where it has a function in recognizing the phage DNA during bacteriophage assembly. Attenuated total reflection FTIR spectroscopy was used to determine the orientation of gene 9 protein in the membrane, revealing that the α-helical domain is mainly transmembrane. The conformational and orientational measurements result in two models for the gene 9 protein in the membrane: a single transmembrane helix model and a two-helix model consisting of a 15 amino acid long transmembrane helix and a 10 amino acid long helix oriented parallel to the membrane plane. Potential structural consequences for both models are discussed.

Keywords: M13; Minor coat protein; Membrane protein orientation; Protein conformation; FTIR

1. Introduction

The filamentous bacteriophage M13 consists of a circular single-stranded DNA molecule of 6408 nucleotides encapsulated in a long cylindrical protein coat. The coat is composed of about 2700 copies of the major coat protein, the product of gene 8. One end of the phage contains about five copies each of the protein products of gene 7 and gene 9. The primary structures of the phage-encoded proteins were deduced from the nucleotide sequence of the DNA genome. Detailed descriptions of the phage particle, the reproductive cycle, and assembly can be

Abbreviations: ATR-FTIR, attenuated total reflection Fourier transform infrared; CD, circular dichroism; *R*, dichroic ratio; DMPC, 1,2-dimyristoyl-*sn*-glycero-3-phosphocholine; DMPG, 1,2-dimyristoyl-*sn*-glycero-3-phosphoglycerol; DOPC, 1,2-dioleoyl-*sn*-glycero-3-phosphocholine; DOPG, 1,2-dioleoyl-*sn*-glycero-3-phosphoglycerol; DPPC, 1,2-dipalmitoyl-*sn*-glycero-3-phosphoglycerol; DSC, differential scanning calorimetry; FTIR, Fourier transform infrared; HPSEC, high performance size exclusion chromatography; L/P, lipid to protein molar ratio; TFA, trifluoroacetic acid; TFE, trifluoroethanol

* Corresponding author. Fax: +31-317-482725;
E-mail: chantal.houbiers@virus.mf.wau.nl

0005-2736/01/$ – see front matter
PII: S0005-2736(00)00369-2

found in several reviews [1–7]. New phage particles are assembled and extruded from its host *Escherichia coli* at the membrane-bound assembly site, without lysis of the host cell. In the assembly site, coat proteins as well as non-structural proteins are present, and the viral DNA is extruded through the cellular membranes while picking up the coat proteins.

Gene 7 and gene 9 proteins were proposed to be associated with the membrane, prior to assembly, based on the finding that they retain their amino-terminal formyl group [8]. Simons et al. [8] suggested that gene 7 and gene 9 proteins are incorporated in phage as primary translational products, so no proteolytic processing occurs. Endeman and Model [9] showed indeed that the gene 7 and gene 9 proteins are localized in the *E. coli* inner membrane prior to assembly.

Gene 7 and gene 9 proteins might play an important initiation role by interacting with the packaging signal of the phage genome [10]. This is supported by the fact that gene 7 and gene 9 proteins are located at the end of the phage particle that emerges first [1]. It was also found that deletions in the packaging signal could be compensated for by mutations in gene 1, gene 7, and gene 9 proteins [10], suggesting a key role for these proteins early in the assembly process. Furthermore, absence of gene 7 or gene 9 protein almost completely abolishes the production of phage particles [1].

In this investigation we focus on the gene 9 protein. The amino acid sequence of this 32 residue protein is the following [11]: HCO-Met-Ser-Val-Leu-Val-Tyr-Ser-Phe-Ala-Ser-Phe-Val-Leu-Gly-Trp-Cys-Leu-Arg^{+}-Ser-Gly-Ile-Thr-Tyr-Phe-Thr-Arg^{+}-Leu-Met-Glu^{-}-Thr-Ser-Ser-COOH. The N-terminal methionine contains the formyl group [8]. To understand more about the role of this protein in assembly, knowledge about its membrane-bound state prior to assembly is of key importance. Hydropathy analysis of the amino acid sequence shows that there is a hydrophobic stretch at the N-terminal side, which runs from residue 1 to around 16, as has been shown before [12]. In addition, we calculated a prediction for an amphipathic helix by Eisenberg's method [13] and found a stretch running from residue 16 to 31. We also searched for predicted turns, using the method of Chou and Fasman [14]. This resulted in two areas with a very high turn potential, which were from residue 17 to 20, and from residue 29 to 32. These predictions are depicted in Fig. 1. Recently the secondary structure of synthetic gene 9 protein was found to be mainly α-helical in 2,2,2-trifluoroethanol (TFE), detergent micelles, and in vesicles of 1,2-dioleoyl-*sn*-glycero-3-phosphoglycerol (DOPG), provided that care was taken to prevent aggregation into β-sheet structures [12]. Based on this information, the membrane-bound conformation of the gene 9 protein was proposed to be predominantly α-helical. In this work we attempt to gain information about how the gene 9 protein is assembled in membranes composed of various lipids. By Fourier transform infrared (FTIR) spectroscopy we determined the orientation of the α-helical domain of gene 9 protein with respect to the membrane plane. In addition, FTIR band analysis revealed

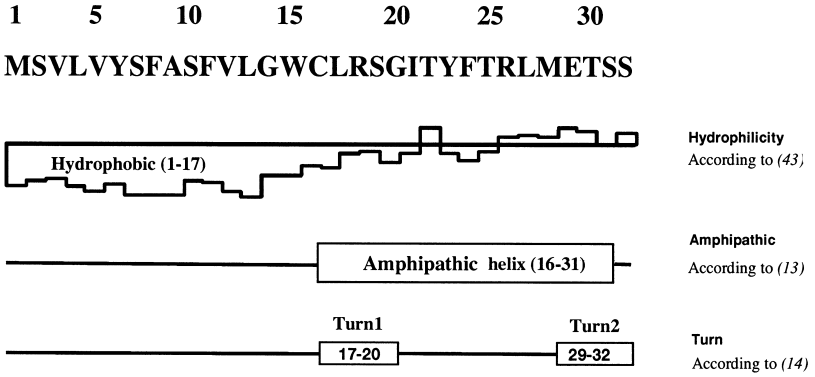

Fig. 1. (A) Hydrophobicity analysis of gene 9 protein according to [43], using a sliding window of 9. (B) Amphipathicity analysis of the gene 9 amino acid sequence by Eisenberg's method [13]. (C) Turn prediction for the gene 9 protein by the method of Chou and Fasman [14].

new features about the secondary structure in the non-helical domain. Altogether, these conformational and orientational measurements result in new models of the gene 9 protein inserted in membranes.

2. Materials and methods

2.1. Materials

9-Fluorenylmethoxycarbonyl amino acids and the solid support *p*-alkoxybenzyl alcohol resin (Wang resin) were purchased from Bachem (Bubendorf, Switzerland). The compounds 1-hydroxybenzotriazole, diisopropylcarbodiimide, and ethanedithiol were obtained from Fluka (Buchs, Switzerland). Dichloromethane, dimethylformamide, isopropyl alcohol, piperidine, and trifluoroacetic acid (TFA) were obtained from Merck (Darmstadt, Germany), and TFE was obtained from Acros (Pittsburgh, PA, USA). DOPG, 1,2-dioleoyl-*sn*-glycero-3-phosphoethanolamine, 1,2-dioleoyl-*sn*-glycero-3-phosphocholine (DOPC), 1,2-dimyristoyl-*sn*-glycero-3-phosphocholine (DMPC), and 1,2-dimyristoyl-*sn*-glycero-3-phosphoglycerol (DMPG) were obtained from Avanti Polar Lipids (Alabaster, AL, USA). The Superdex 75 column was obtained from Pharmacia (Uppsala, Sweden). The gene 9 protein was prepared by solid phase synthetic techniques and characterized as described before [12]. The N-terminus was synthesized with a formyl group.

2.2. Solubilization of protein in TFE

The protein was first dissolved in a small volume of TFA (10–20 μl/mg protein) and dried under a stream of nitrogen. Next, the protein was washed two times with TFE, followed by evaporation of the TFE under a stream of nitrogen to remove residual TFA. Finally the protein was dissolved in a known volume of TFE. To remove residual traces of TFA (which can contribute to the signal in the amide I region in FTIR measurements [15]), a 2 mM HCl solution was added to the TFE stock in a 1/1 (v/v) ratio, to yield a 1 mM HCl concentration in the protein solution. The solution was subsequently lyophilized, redissolved into TFE, and used for further sample preparation. The protein concentration was determined by the procedure of Peterson [16] with bovine serum albumin as a standard.

2.3. Reconstitution of protein into lipid vesicles

A desired amount of phospholipid was taken from a chloroform solution in the case of dioleoyl lipids. The chloroform was evaporated under a stream of nitrogen, and the remaining lipid film was kept overnight under vacuum to remove all traces of chloroform. In the case of dimyristoyl lipids the desired amount was weighed as a powder. To reconstitute the gene 9 protein in the lipids, the method described by Killian et al. [17] was used. Briefly, the desired amount of gene 9 protein dissolved in TFE was added to an equal volume of water, containing the desired amount of lipids. The mixture was vortexed for 2 s at room temperature. Next, this mixture was diluted to yield a 16:1 ratio of water to TFE by volume. The samples were mixed by vortexing for 2 s and lyophilized. The sample was rehydrated in the desired volume of water.

2.4. Sucrose gradient centrifugation

Samples of reconstituted proteins in DOPC or DOPG were placed on top of a linear 0–40% w/w sucrose gradient, and centrifuged for 18 h at $110\,000 \times g$ at 4°C in a Beckman SW41 rotor. To enable visualization of the lipid–protein complexes, octadecyl rhodamine B (0.16% mol/mol lipid) was added, which dissolves into the membranes with high specificity.

2.5. Differential scanning calorimetry (DSC)

Gene 9 protein in 1,2-dipalmitoyl-*sn*-glycero-3-phosphoglycerol (DPPC) vesicles were prepared by mixing a known amount of protein solubilized in TFE with 5 mg of DPPC dissolved in chloroform. After evaporation of the solvent the samples were dried under vacuum for 3 h and resuspended in 750 μl 50 mM Tris, pH 8.0. After homogenization the liposomes were collected by low speed centrifugation and redissolved in 30 μl of buffer. 20 μl of this sample was used in a 25 μl cup for DSC. Samples were measured using a Pyris 1 DSC (Perkin-Elmer) at a heating rate of 10°C/min. From the heating

scans the phase transition temperature and peak width were determined.

2.6. Determination of the aggregation state of the protein

The aggregation state of the gene 9 protein samples was checked after FTIR measurements. The samples were diluted 15 times with cholate elution buffer (50 mM cholate, 10 mM sodium phosphate, 20 mM NaCl, pH 8.0) to dissolve the lipid vesicles and immediately analyzed after addition of the cholate. High performance size exclusion chromatography (HPSEC) was performed on a Superdex 75 column (1.0×30 cm). A flow of 0.5 ml/min was applied in the cholate elution buffer mentioned above. Online detection was done by fluorescence measurement. For molecular weight calibration of the columns, alcohol dehydrogenase (150 000 Da), bovine serum albumin (67 000 Da), myoglobin (18 800 Da), A-protinin (6500 Da), and bacitracin (1400 Da) were used.

2.7. FTIR spectroscopy

Samples for FTIR typically contained 0.04 mg protein at a lipid/protein (L/P) ratio of 25 (mol/mol). Films were prepared on a CaF_2 window (13 mm diameter). FTIR spectra were recorded on a Perkin-Elmer 1750 FTIR spectrometer at room temperature. The optical bench was purged with dry air (Balston, Maidstone, UK) at a flow rate of 25 l/min. The acquisition parameters were the following: 4 cm^{-1} resolution; 32 co-added interferograms, 3500–900 cm^{-1} wavenumber range. For the sake of comparison, spectral intensities were normalized with the maximum peak in the amide I region, after subtraction of a straight baseline passing through the two minima bordering the amide I region. Partially dehydrated films were prepared by keeping the samples, spread as a suspension on the CaF_2 window, for several hours in a cabin continuously purged with dry air. Samples were mounted in the FTIR spectrometer without exposure to the room air by using a rubber spacer and a second CaF_2 window to cover the sample film. Deuterated samples were prepared similarly, but were immersed in 40 μl D_2O before drying for several hours in the cabin purged with dry air. Before measurement 3 μl of D_2O was added on top of the dried film, which was enough to fully immerse the film in D_2O during the measurement. A second CaF_2 window was used to cover the sample.

2.8. Attenuated total reflection (ATR)-FTIR spectroscopy

Oriented multibilayers were formed by slow evaporation of a 15 μl sample, containing 0.03 mg protein and the lipids, on one side of the ATR plate, which was placed in a sample holder (Perkin Elmer 186-0354). Spectra were recorded at room temperature on a Perkin-Elmer infrared spectrophotometer 1720X equipped with a Perkin-Elmer microspecular reflectance accessory and a polarizer mount assembly with a gold wire grid element. The internal reflection element was a germanium ATR plate (50×20×2 mm, Harrick EJ2121) with an aperture angle of 45° yielding 25 internal reflections. 128 accumulations were performed to improve the signal/noise ratio. The spectrophotometer was continuously purged with dried air (FTIR purge gas generator 75-62, Whatman, Haverhill, MA, USA). Spectra were recorded at a nominal resolution of 2 cm^{-1}. Remaining spikes due to H_2O vapor were subtracted as described before [18]. Subsequently, the spectra were smoothed by apodization of the Fourier-transformed spectrum by a Gaussian lineshape with a full width at half height of 4 cm^{-1}.

2.9. Orientation of the secondary structures

In an α-helix, the main transition dipole moment lies approximately parallel to the helix axis. It is therefore possible to determine the mean orientation of the α-helix structure from the orientation of the peptide bond C=O group [19]. Spectra were recorded with parallel and perpendicular polarized incident light with respect to the incidence plane. The dichroic spectra are the difference between the spectra recorded with parallel and perpendicular polarizations. The perpendicular spectra were multiplied by a factor R_{iso} (i.e., the dichroic ratio for an isotropically oriented sample) before subtraction to take into account the difference in the relative power of the evanescent fields [20]. This is allowed since the C=O groups of the phospholipids are assumed to

have no net orientation [20]. Polarization was expressed as the dichroic ratio R. R is defined as the ratio $A_{\parallel}/A_{\perp}$, where $A_{\parallel}$ and $A_{\perp}$ are the absorbances (measured as band areas) with the parallel and perpendicular orientations of the polarizer. The dichroic ratio was converted into an order parameter, which can be related to a maximum tilt angle θ of an orientational distribution of dipoles [19,20]. The angle θ is defined as the maximum angle of the molecular (helix) axis with respect to the normal of the ATR plate. For the amount of material used throughout this work, film thickness (0.1–0.3 μm) is small when compared to the IR wavelength (6.06 μm at 1650 cm^{-1}), but close to the penetration depth d_p (0.39 μm). This does not allow the 'thin film' approximation [19] to be used, but instead the film thickness has to be taken into account for the establishment of the equations describing the dichroic ratio as a function of the orientational order parameter [20]. This can be achieved by computing an apparent film thickness from R_{iso}), using $n_1 = 4.0$ (germanium), $n_2 = 1.7$ (protein), $n_3 = 1.0$ (air) in order to evaluate correctly the electric field component perpendicular to the ATR plate [20]. The angle between the long axis of the α-helix and the (C=O) dipole moment was taken as 27° [19,21].

2.10. Secondary structure determination

Curve fitting with Lorentzian lines was performed with the software Origin 4.0. The position of the bands was chosen on the basis of the shape of the deconvoluted spectra. Fourier self-deconvolution was used using a Lorentzian line shape (full width at half height = 30 cm^{-1}) and a Gaussian line shape (full width at half height = 15 cm^{-1}) for the apodization. This procedure has been detailed elsewhere [19,22,23]. Intensity, width, and frequency of the Lorentzian bands were adjusted by the program. To avoid contributions of the lipid C=O vibration in the amide I region, we removed the lipid C=O band around 1740 cm^{-1} by subtracting the pure lipid spectrum after scaling on the lipid C=O band prior to curve fitting. A straight baseline was adjusted as an additional parameter to obtain the best fit. After band fitting each component was assigned to a secondary structure type, and then the integrated areas of these components were expressed as a percentage of the total amide I area and were used to determine the secondary structure elements [22].

3. Results

3.1. Reconstitution of protein in lipid vesicles

Gene 9 protein was reconstituted in phospholipid vesicles via the method of cosolubilization with organic solvent [17], which was shown to be a proper method for the gene 9 protein [12]. Binding of the gene 9 protein to DOPC and DOPG vesicles was checked by sucrose density gradient centrifugation. All protein was bound to lipids (data not shown). This was concluded from the observation of a lipid–protein band at intermediate position in the centrifugation tube, whereas no bands were observed at the top of the tube where, in control experiments, pure lipid vesicles end up, or at the bottom of the tube where the pure proteins were located. In order to check whether the lipid acyl chains were influenced by the gene 9 protein, we studied gene 9 protein reconstituted in lipids by DSC. As a membrane model system we used DPPC, which has a phase transition at 42°C. When DPPC vesicles contained gene 9 protein the phase transition shifted to lower temperature and broadened (data not shown). Upon increasing the gene 9 protein concentration the effect was more pronounced. These results indicate that the lipid acyl chains are influenced by the presence of protein. However, by using FTIR we found that the acyl chains at room temperature were not greatly disturbed by the presence of protein in DMPC, DMPG, DOPC, and DOPG phospholipids. This is concluded from the observation that the acyl chain stretch vibrations of the lipids around 2925 and 2854 cm^{-1} show only a very small shift in the lipid C=O stretching, which could result from a slightly different hydration of the carbonyl of the lipid heads, with or without gene 9 protein reconstituted in the membrane (data not shown).

3.2. Conformation

Fig. 2 (curve A) shows the 1800–1400 cm^{-1} region of the FTIR spectrum of gene 9 protein in DMPG. The lipid (C=O) band is found at 1738 cm^{-1}, the

protein amide I at 1657 cm^{-1} and amide II at 1546 cm^{-1}. The lipid contribution was removed by subtraction of the FTIR spectrum of pure lipid contribution in Fig. 2C. The resulting difference spectrum (curve C) shows a wiggle with a negative and a positive intensity centered around the position of the lipid C=O band. This indicates that in the presence of protein the lipid (C=O) band experience a slight shift to higher wavenumbers.

Since the amide I band (1600–1700 cm^{-1}) is most useful for structure determination, Fig. 3 compares the amide I regions of the FTIR spectra of gene 9 protein in three different lipid systems with dimyristoyl acyl chains: DMPC, DMPC/DMPG (3/1, mol/mol), and DMPG (the latter as taken from graph A of Fig. 2). Similar bandshapes were obtained for three different lipid systems with dioleoyl acyl chains: DOPC, DOPC/DOPG, and DOPG (data not shown). All these lipid systems, varying in head group composition (neutral PC versus negatively charged PG head group) and in acyl chain composition (saturated dimyristoyl versus unsaturated dioleoyl acyl chains), result in similar amide I bands of gene 9 protein reconstituted in these systems.

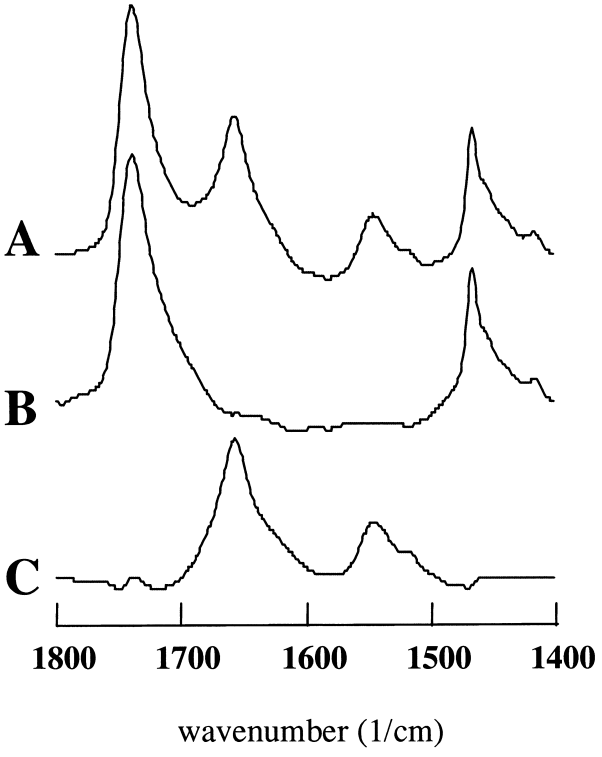

Fig. 2. FTIR absorption spectra of partially dehydrated films of gene 9 protein reconstituted in DOPG at an L/P ratio of 25 (mol/mol) (A) and of identically treated DOPG without protein (B). In the lower spectrum (C), spectrum B is subtracted from A after normalization on the areas of the lipid C=O band, to remove the contribution of the lipids.

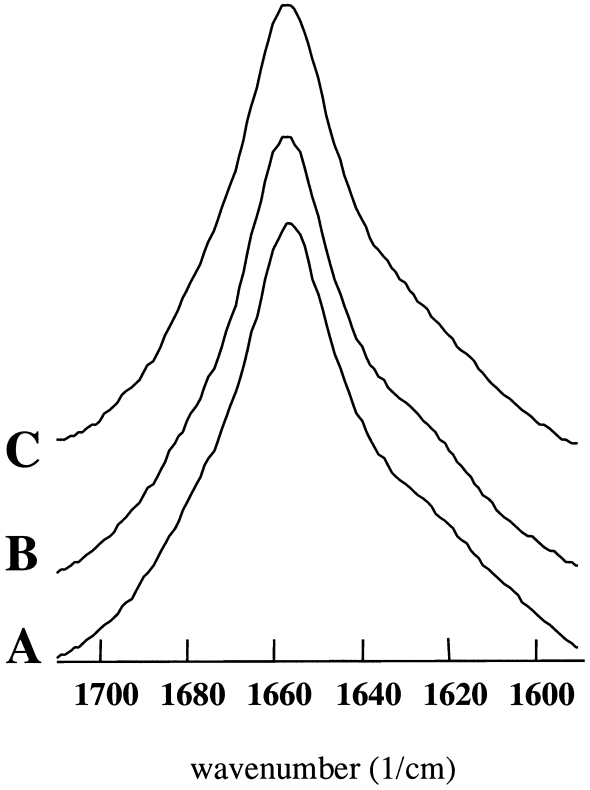

Fig. 3. Amide I region of the FTIR absorption spectra of partially dehydrated films of gene 9 protein reconstituted in DMPC (A), DMPC/DMPG (3/1, mol/mol) (B), DMPG (C). Lipid contributions have been subtracted as shown in Fig. 2. L/P ratios were 25 (mol/mol).

Deconvolution of the spectra, as shown in Fig. 4C for gene 9 protein in DMPC/DMPG (3/1, mol/mol), identifies the presence of three components located around 1679, 1657, and 1627 cm^{-1}. Curve fitting (e.g., Fig. 4A), was used to quantify the relative contributions of the three bands. The difference spectrum between the original spectrum and the fit is presented in Fig. 4B. Curve fitting results obtained for the gene 9 protein in the dimyristoyl lipid series and the assignments are presented in Table 1. The results for the dioleoyl lipids (not shown) are very similar.

The main band at 1657 cm^{-1} is assigned to α-helix

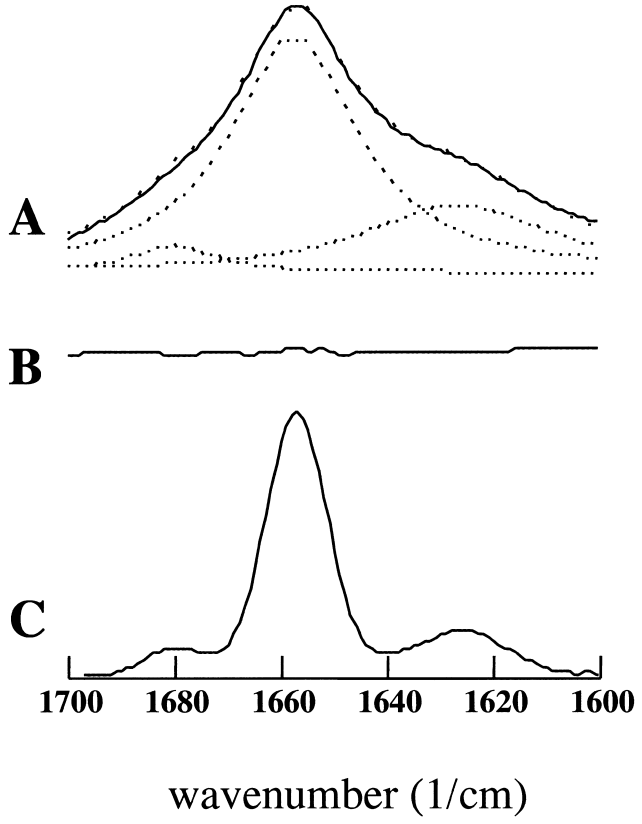

Fig. 4. (A) FTIR absorption spectrum of a partially dehydrated film of gene 9 protein reconstituted in DMPC/DMPG (3/1, mol/mol) after lipid subtraction (solid line) and the component spectra (dashed lines) that are used to fit the spectrum according to the parameters given in Table 1. The total fit is represented by dashes. (B) Difference of the absorption spectrum and the sum of the fitted component spectra in A. (C) Deconvoluted spectrum.

[18]. The relatively narrow bandwidth agrees with a major contribution of α-helical absorption. Since it is known that random coil contribution overlaps the α-helical absorption in films or H_2O suspension [24,25] we also measured the samples in dioleoyl lipids in D_2O suspension after exposure to D_2O for several hours. Random coil structure is known to exchange hydrogen for deuterium on a fast timescale, resulting in a shift of the amide I band to approximately 1640 cm^{-1} [18,24–26]. We did not observe such a shift. The amide I band was shifted only 1–3 cm^{-1} to lower wavenumber and the loss of amide II intensity was very small confirming the α-helix assignment. Furthermore, the very slow exchange rate indicates that the helix structure is either extraordinarily stable or embedded in the hydrophobic region of the lipid membrane. In addition, we measured these samples by circular dichroism (CD; data not shown). All spectra were similar to the CD spectrum of gene 9 protein in DOPG [12], indicating the secondary structure of gene 9 protein is mainly α-helical. Nor did CD measurements indicate any β-sheet structure, showing a zero crossing around 202–203 nm for all samples. The presence of β-sheet would shift the zero crossing up to 210 nm [27].

The bands around 1627 and 1679 cm^{-1} are assigned to turn structure. HPSEC analysis of these samples did not show the presence of any aggregated protein (data not shown), which has been shown to correspond with β-sheet structure [12]. Thus, the presence of only monomeric protein excludes β-sheet

Table 1
Analysis of the amide I region of gene 9 protein in various lipid systems[a]

Lipid system	Unpolarized spectra			Assignment	Dichroic spectra (∥−⊥)		
	γ (cm^{-1})	$\Delta\gamma$ (cm^{-1})[b]	area (%)[c]		γ (cm^{-1})	$\Delta\gamma$ (cm^{-1})[b]	area (%)[c]
DMPC	1679	20	6	hydrogen-bonded turn	1680	13	4
	1657	29	61	α-helix	1657	25	90
	1625	49	33	non-hydrogen-bonded turn	1635	18	6
DMPC/DMPG (3/1, mol/mol)	1680	18	5	hydrogen-bonded turn	1680	18	8
	1657	29	67	α-helix	1659	22	86
	1627	42	28	non-hydrogen-bonded turn	1637	20	6
DMPG	1678	17	5	hydrogen-bonded turn	1678	22	11
	1657	29	69	α-helix	1659	23	84
	1627	43	26	non-hydrogen-bonded turn	1636	17	5

[a]The error on the frequency γ and linewidth $\Delta\gamma$ is ± 2 cm^{-1}.
[b]Full width at half height
[c]Relative area in amide I. The error in the calculated area is $\pm 5\%$.

structure, since the monomeric state corresponds to a predominant α-helical structure [12]. Therefore, the FTIR bands around 1627 and 1679 cm^{-1} can be assigned to turn structure, and not to β-sheet structure. Based on previous work [28,29] the low wavenumber band around 1627 cm^{-1} is assigned to hydrogen-bonded groups present in a turn structure, whereas the high wavenumber band around 1679 cm^{-1} is assigned to the non-hydrogen-bonded C=O groups present in a turn structure [28–30]. On the basis of this assignment, the total amount of turn structure then amounts to 35 ± 5%. Quantification in this way supposes that the extinction coefficients do not vary with secondary structure type. However, the literature shows that this may not be the case [31]. In that case the band at 1685 cm^{-1} would be underestimated, and the band at 1630 cm^{-1} would be similarly to some extent overestimated with respect to the α-helix content. The assignment of the bands around 1627 and 1679 cm^{-1} to turn structure is in agreement with the results found for bacteriophage M13 major coat protein. This protein yielded similar FTIR bands, which were assigned to turn structures because the ratio of the two bands did not correspond to the ratio of 10 expected for β-sheet [30]. Byler and Susi [24] assigned similar bands at 1675 and 1638 cm^{-1} for several highly helical proteins (hemoglobin, myoglobin, cytochrome *c*, and ferritin) and assigned these to the short extended chains connecting the helical cylinders (and not to β-sheet). Haris et al. [32] observed similar bands in rhodopsin in bovine rod outer segment membranes, which were assigned to turn structures.

We checked for amino acid side chain contributions in our spectra by calculating the contributions from the tyrosine, arginine, glutamic acid, and phenylalanine residues present in gene 9 protein (data not shown). These side chains contribute in the amide I and amide II regions [33]. Subtraction of these contributions from our spectrum does not significantly influence spectral intensities and lineshapes.

3.3. Orientation

To determine the orientation of the gene 9 protein in lipid bilayers by ATR-FTIR spectroscopy the phospholipid membrane should be well ordered. For this reason we used the dimyristoyl lipids instead of the dioleoyl lipids. In addition, the saturated acyl chains of the dimyristoyl lipids allow an accurate orientation determination of the lipids by means of the $\gamma_w(CH_2)$ progression [34].

For gene 9 protein reconstituted in DMPC, DMPC/DMPG (3/1, mol/mol), and DMPG vesicles spectra were recorded with incident light polarized parallel or perpendicular to the incidence plane. The dichroic spectra are the difference between the spectra recorded with parallel and perpendicular polarizations, as described in Section 2. Fig. 5 shows the ATR-FTIR spectra of the gene 9 protein reconstituted in DMPC/DMPG (3/1, mol/mol) for parallel and perpendicular orientations of the polarizer (lower spectra) and the dichroic spectrum (top). The dichroic spectrum in Fig. 5 demonstrates a positive deviation, indicating that the dipole is oriented

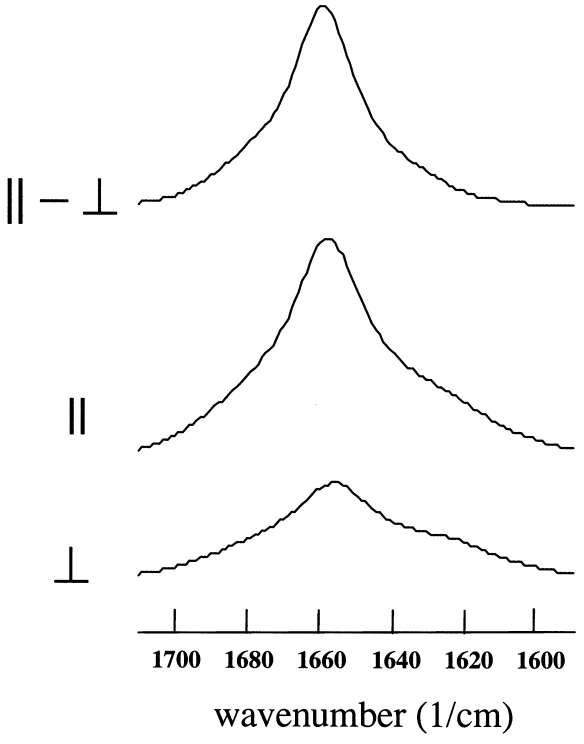

Fig. 5. ATR-FTIR spectra of gene 9 protein reconstituted in DMPC/DMPG (3/1, mol/mol), partially dehydrated, for parallel and perpendicular orientations of the polarizer. The dichroic spectrum (top) was obtained as ∥ minus ⊥ spectrum after multiplication of the ⊥ spectrum by R_{iso} (see Table 2). It should be noted that the intensity of the dichroic spectrum (top) was expanded twice for better visualization. The L/P ratio was 25 (mol/mol).

Table 2
Dichroic ratio values of amide I and corresponding maximum tilt angles for gene 9 protein in various lipid systems

Lipid system[a]	R^b	R_α^b	R_{iso}^b	θ (°)[c]	x^d
DMPC	1.72	1.96	1.18	33	0.61
DMPC/DMPG (3/1, mol/mol)	2.06	2.43	1.241	30	0.70
DMPG	2.06	2.48	1.20	27	0.77

[a]The L/P ratios were 25 (mol/mol). The lipid contribution was subtracted from both spectra with the parallel and perpendicular orientations of the polarizer as was performed in Fig. 2.
[b]R is the dichroic ratio; R_α is the dichroic ratio for the helix component and R_{iso} the dichroic ratio for an isotropically oriented sample.
[c]One-helix model assuming 100% helix. The error in the calculated angles is $\pm 5°$.
[d]Two-helix model. x is the fraction of transmembrane helix relative to the total helix content.

mainly parallel to the normal of the plate. Since in an α-helix the amide I dipole is close to the helix long axis [19] this result demonstrates that the helix axis is oriented mainly parallel to the normal of the ATR plate. Nearly identical results were obtained for the gene 9 protein reconstituted in DMPC or in DMPG (spectra not shown).

From Fig. 5 it can be noted that bandwidth in the dichroic spectrum is smaller than the bandwidth of the unpolarized spectra. Analysis of the component bands (Table 1) shows that the bands assigned to turn contribute much less in the dichroic spectra, whereas the α-helix band is more predominant (up to 90% contribution). The relatively lower prevalence of the turn bands in the dichroic spectrum indicates that these structures are less oriented, whereas the α-helical structure adopts a strong orientation. The absence of the non-helical structures (turns, random) in the polarized spectra explains why the dichroic spectra are narrower.

The orientation of the lipid acyl chains was assessed by means of the $\gamma_w(CH_2)$ progression between 1200 and 1350 cm^{-1}. This band structure originates from a resonance between the CH_2 groups and the ester group of the all-*trans* hydrocarbon chain in the α-position (peaks at 1202, 1227, 1254, 1278, 1304, and 1327 cm^{-1}) [34]. The strong ∥ polarizations of these peaks, and therefore their positive deviations in the dichroic spectrum (data not shown), indicates that the all-*trans* hydrocarbon chains of DMPC are nearly normal to the germanium surface. This implies that the membranes are highly oriented parallel to the ATR plate and that the helix of the gene 9 protein is oriented preferentially perpendicular relative to the membrane plane.

The orientation of dipoles can be analyzed in a more quantitative way by considering dichroic ratio values. The dichroic ratio R, defined as $A_\parallel/A_\perp$, can be converted into an order parameter, which can be converted into the so-called maximum tilt angle θ between the molecular (helix) axis and the normal of the ATR plate ([20]). In our calculations we assume perfect membrane ordering, resulting in an order parameter of 1.0. This assumption is justified by the observation of a very high degree of orientation of the lipid molecules. Dichroic ratios of the $\gamma_w(CH_2)$ progression bands of the all-*trans* hydrocarbon chains of the lipids between 1300 and 1200 cm^{-1} yielded values in the range from 3 to 6. This indicates that the all-*trans* hydrocarbon chains were oriented nearly normal to the germanium surface [34,35], irrespective of whether protein was present or not. This observation implies an almost perfect membrane order. The dichroic ratios calculated from the amide I bands of the ATR-FTIR spectra of gene 9 protein reconstituted in DMPC, DMPC/DMPG (3/1, mol/mol), and DMPG for parallel and perpendicular orientations of the polarizer are presented in Table 2. The third column shows values for R_{iso} which were used to calculate the real film thickness, which is required for the orientation determination [20]. The fourth column shows the calculated maximum tilt angle θ of the helix according to Raussens et al. [36].

4. Discussion

Gene 9 protein is known to be located in the inner membrane of *E. coli* before incorporation into bacteriophage M13 [9]. A first characterization of the

gene 9 protein in the membrane-bound state was performed in model membrane systems including organic solvent, detergent micelles, and phospholipid vesicles [12]. The gene 9 protein was found to be mainly α-helical and the percentage of α-helix was estimated based on CD measurements. In this paper we aimed to determine how the gene 9 protein is located in the membrane by measuring the orientation of the α-helical domain in the bilayer, using FTIR spectroscopy. In addition, we performed a quantitative analysis of the components of the FTIR amide I band, resulting in new information on secondary structure of the gene 9 protein.

4.1. Reconstitution of protein in lipid vesicles

First we established that the gene 9 protein was incorporated in the phospholipid bilayers. The gene 9 protein was reconstituted in phospholipid vesicles by using a protocol of cosolubilization with organic solvent [17], which has also been shown to be applicable for the gene 9 protein [12]. After reconstitution protein–lipid complexes were analyzed by sucrose density centrifugation to determine whether all protein was complexed to the lipids. The observation of one band at intermediate density, indicating a mix of proteins and lipids, and no protein band at high density or lipid band at low density, indicated that all protein was complexed with the phospholipid vesicles, and that no free protein was present. Using DSC the effect of protein incorporation on the phase transition temperature of DPPC acyl chains was monitored. The observation that gene 9 protein causes a shift and a broadening of this phase transition indicates that the protein must be influencing the lipid acyl chains. We concluded that the protein is not just bound to the surface of the membrane, but must be penetrating into the interior of the membrane [37]. These observations indicate that in the experiments carried out after reconstitution the gene 9 protein was at least partly incorporated in the bilayer interior, and not just peripherally bound to the surface of the membrane.

4.2. Conformation

Analysis of the amide I regions of the infrared spectra of gene 9 protein in DOPC, DOPC/DOPG (3/1, mol/mol), DOPG, DMPC, DMPC/DMPG (3/1, mol/mol), and DMPG (Figs. 3 and 4) shows that it consists of three bands. The main band, representing 67% of the area, at 1657 cm^{-1} is assigned to α-helix [18,24]. This assignment is supported by measurement of the samples in D_2O, and by CD measurements. Apparently, the protein contains similar amounts of α-helix irrespective of the head group charge or acyl chain saturation. The percentage of α-helix found here is slightly higher than reported before [12].

The dichroic spectra (Fig. 5), resulting from the orientation measurements, and the analysis of their component bands (Table 1) provide additional information. The bands around 1627 and 1679 cm^{-1} have a net positive, but much smaller, deviation in the dichroic spectrum than in the unpolarized spectrum. This agrees with turn structure, since turns are expected to have a less defined orientation than α-helices. HPSEC and CD measurements support the conclusion that the presence of β-sheet can be ruled out. On the basis of this assignment the total amount of turn structure then increases to 31–39%. Gene 9 protein contains 32 amino acids, so it is possible that gene 9 protein might contain two turns, each of about five amino acids, as already suggested by the turn prediction [14].

4.3. Orientation

To our knowledge the only detailed information available about the membrane-bound state of the gene 9 protein describes conformational properties [12]. Nothing is known about how gene 9 protein is assembled in the lipid membrane. Here we provide additional information by measuring the orientation of gene 9 protein in lipid bilayers, deposited on germanium plates by ATR-FTIR spectroscopy. In an α-helix the transition dipole moment of the amide I band lies approximately parallel to the helical axis, so it is possible to determine the mean orientation of an α-helix from the orientation of the C=O group [19]. Dichroic spectra, allowing a qualitative analysis of the orientation, of the gene 9 protein in DMPC, DMPC/DMPG (3/1), and DMPG show a positive band at 1657 cm^{-1}, indicating that the α-helix is oriented preferentially parallel to the membrane normal. The turn structure, assigned to the peaks

around 1680 and 1630 cm^{-1}, is less well oriented as judged from their relatively weaker contributions in the dichroic spectra (Table 1).

Assuming that the membranes are perfectly ordered, the dichroic data were analyzed quantitatively by calculating the maximum tilt angle (Table 2) [20]. These results indicate that in the different lipid systems the gene 9 protein deviates by a maximum tilt angle of 27–33° from the membrane normal. In the presence of membrane disorder, this angle is reduced, so on average the helix axis may be closer to the membrane normal. Until now we have assumed in the calculations of the orientation that the protein is fully α-helical. Therefore we also calculated the maximum tilt angle in the case that a fraction of 67% of the molecule is α-helical, as found in Table 1 for the DMPC/DMPG system. In this calculation it is assumed that the remaining protein part has no net orientation. This is a reasonable assumption, since turn structures hardly show up in the dichroic spectrum (Fig. 5 and Table 1), and therefore are not well oriented. By this correction the dichroic ratios of the α-helix component (R_α), as given in Table 2, show a reduction of the maximum tilt angle by about 5°. This leads to a maximum tilt angle of approximately 28°.

4.4. Model of gene 9 protein in membranes and biological implications

Summarizing, we conclude from Table 1 that the gene 9 protein conformation is about 67% α-helical, and that the remaining part consists mainly of turn structure. The α-helical part adopts a preferentially transmembrane orientation with calculated maximum tilt angles as shown in Table 2. If we interpret this result assuming a single α-helical strand in the gene 9 protein, this implies that the helix has a length of about 21 residues and is maximally tilted up to 28° from the membrane normal. This value compares well with the results found for the single membrane spanning major coat protein of bacteriophage M13 [38]. Combining this model with hydrophobicity data (Fig. 1), it appears that the helix is located at the N-terminus. This implies that Trp^{15} is not at the interface, but is located more to the center of the membrane, and Arg^{18} is positioned within the transmembrane helix. Similar to the lysine residues in gene 8 protein of bacteriophage M13 [39], Arg^{18} might function as an anchor of one end of the helix. The turn structure must be located at the C-terminus, facing the aqueous phase.

An alternative interpretation can be made when the measured dichroic ratio is assumed to be the average of the dichroic ratios of two highly oriented helices within one protein: one transmembrane helix, and a second helix parallel to the membrane plane. The fraction (x) of transmembrane helix contribution to the total helix content, indicating the relative length of this helix, can be calculated from the experimental dichroic ratio and the dichroic ratios of perfectly parallelly and perpendicularly oriented helices (Table 2) [40]. This calculation results in a longer helix (about 15 residues) oriented transmembrane, and a shorter helix (about six residues) oriented parallel to the membrane surface.

This two-helix model agrees remarkably well with the prediction of a hydrophobic helix at the N-terminus, which shows one turn connecting the two helices, and another turn at the C-terminus (Fig. 1). This model suggests favorable locations for Trp^{15} and Gly^{20}: Trp^{15} is located around the membrane interface, and Gly^{20} may be involved in a turn structure, which connects the transmembrane and amphipathic helix. However, it also implies that the transmembrane helix is about 15 residues long, which would be too short to fully span a membrane in an α-helical conformation. This problem can partly be relieved by having the amphipathic helix deeply inserted in the polar head group region, anchoring in the hydrophobic region with its hydrophobic residues Phe^{24} and Leu^{27}. In this case the helix may just reach the lipid carbonyl groups on the opposite site of the membrane by its polar formyl group at the N-terminus.

The present spectroscopic results cannot discriminate between the one-helix and the two-helix models. In comparing both models, it can be seen that the largest fraction of the helical region adopts a transmembrane orientation and a turn structure shows up at the C-terminus. The presence of turn structure at the C-terminus may be of importance for the biological function of the gene 9 protein, since turns frequently have been suggested as the bioactive conformation in recognition processes [41,42]. This is supported by the finding that the C-terminal end

plays an important role in the formation of the complex with the DNA hairpin loop of the packaging signal of the phage DNA [10].

Acknowledgements

We are grateful to Folkert Hoekstra and Mark Alberda for the use of the FTIR spectrometer and the stimulating discussions. E.G. is Research Director of the National Fund for Scientific Research (Belgium). This research was supported by the Life Sciences Foundation (SLW) with financial aid of The Netherlands Organization for Scientific Research (NWO).

References

[1] R.E. Webster, J. Lopez, in: S. Casjens (Ed.), Virus Structure and Assembly, Jones and Bartelett, Boston, MA, 1985, pp. 235–267.
[2] I. Rasched, E. Oberer, Microbiol. Rev. 50 (1986) 401–427.
[3] P. Model, M. Russel, in: R. Calender (Ed.), The Bacteriophages, Vol. 2, Plenum Press, New York, 1988, pp. 375–456.
[4] R.E. Webster, in: B. Kay, J. Winter, J. McCafferty (Eds.), Phage Display of Peptides and Proteins, Academic Press, San Diego, CA, 1996, pp. 1–20.
[5] D. Marvin, Curr. Opin. Struct. Biol. 8 (1998) 150–158.
[6] M. Russel, Mol. Microbiol. 5 (1991) 1607–1613.
[7] M. Russel, Trends Microbiol. 3 (1995) 223–228.
[8] G.F.M. Simons, J. Beintema, F.J. Duisterwinkel, R.N.H. Konings, J.G.G. Schoenmakers, Prog. Clin. Biol. Res. 64 (1981) 401–411.
[9] H. Endemann, P. Model, J. Mol. Biol. 250 (1995) 496–506.
[10] M. Russel, P. Model, J. Virol. 63 (1989) 3284–3295.
[11] P. Van Wezenbeek, T. Hulsebos, J. Schoenmakers, Gene 11 (1980) 129–148.
[12] M.C. Houbiers, R.B. Spruijt, C.J.A.M. Wolfs, M.A. Hemminga, Biochemistry 38 (1999) 1128–1135.
[13] D. Eisenberg, R. Weiss, T. Terwilliger, Proc. Natl. Acad. Sci. USA 81 (1984) 140–144.
[14] P. Chou, G. Fasman, Annu. Rev. Biochem. 47 (1978) 251–276.
[15] P.I. Haris, D. Chapman, Biopolymers 37 (1995) 251–263.
[16] G.L. Peterson, Anal. Biochem. 83 (1977) 346–356.
[17] J.A. Killian, T.P. Trouard, D.V. Greathouse, V. Chupin, G. Lindblom, FEBS Lett. 348 (1994) 161–165.
[18] E. Goormaghtigh, V. Cabiaux, J.-M. Ruysschaert, in: H.J. Hilderson, G.B. Ralston (Eds.), Physicochemical Methods in the Study of Biomembranes, Vol. 23, Plenum Press, New York, 1994, pp. 329–450.
[19] E. Goormaghtigh, J.-M. Ruysschaert, in: R. Brasseur (Ed.), Molecular Description of Biological Membranes by Computer Aided Conformational Analysis, Vol. 1, CRC Press, Boca Raton, FL, 1990, pp. 285–329.
[20] B. Bechinger, J.-M. Ruysschaert, E. Goormaghtigh, Biophys. J. 76 (1999) 552–563.
[21] K. Rothschild, N. Clark, Biophys. J. 25 (1979) 473–487.
[22] E. Goormaghtigh, V. Cabiaux, J.-M. Ruysschaert, Eur. J. Biochem. 193 (1990) 409–420.
[23] J.K. Kauppinen, D.J. Moffat, H.H. Mantsch, D.G. Cameron, Appl. Spectrosc. 35 (1981) 271–276.
[24] D. Byler, H. Susi, Biopolymers 25 (1986) 469–487.
[25] W.K. Surewicz, H.H. Mantsch, Biochim. Biophys. Acta 952 (1988) 115–130.
[26] P. Haris, D. Lee, D. Chapman, Biochim. Biophys. Acta 874 (1986) 255–265.
[27] N.J. Greenfield, G.D. Fasman, Biochemistry 8 (1969) 4108–4116.
[28] J. Bandekar, Biochim. Biophys. Acta 1120 (1992) 123–143.
[29] H. Mantsch, A. Perczel, M. Hollosi, G. Fasman, Biopolymers 33 (1993) 201–207.
[30] W.F. Wolkers, P.I. Haris, A.M.A. Pistorius, D. Chapman, M.A. Hemminga, Biochemistry 34 (1995) 7825–7833.
[31] H.H. de Jongh, E. Goormaghtigh, J.-M. Ruysschaert, Anal. Biochem. 242 (1996) 95–103.
[32] P. Haris, M. Coke, D. Chapman, Biochim. Biophys. Acta 995 (1989) 160–167.
[33] S. Venyaminov, N. Kalnin, Biopolymers 30 (1990) 1243–1257.
[34] U. Fringeli, and H. Gunthard, in: E. Grell (Ed.), Membrane Spectroscopy, Vol. 31, Springer, Berlin, 1981, pp. 270–332.
[35] V. Raussens, V. Narayanaswami, E. Goormaghtigh, R.O. Ryan, J.M. Ruysschaert, J. Biol. Chem. 270 (1995) 12542–12547.
[36] V. Raussens, J.-M. Ruysschaert, E. Goormaghtigh, J. Biol. Chem. 272 (1997) 262–270.
[37] I. Azpiazu, J.C. Gomez-Fernandez, D. Chapman, Biochemistry 32 (1993) 10720–10726.
[38] C. Glaubitz, G. Grobner, A. Watts, Biochim. Biophys. Acta 1463 (2000) 151–161.
[39] D. Stopar, R.B. Spruijt, C.J.A.M. Wolfs, M.A. Hemminga, Biochemistry 35 (1996) 15467–15473.
[40] E. Goormaghtigh, V. Raussens, J.-M. Ruysschaert, Biochim. Biophys. Acta 1422 (1999) 105–185.
[41] J. Smith, L. Pease, CRC. Crit. Rev. Biochem. 8 (1980) 315–399.
[42] A. Perczel, M. Hollosi, in: G. Fasman (Ed.), Circular Dichroism and the Conformational Analysis of Biomolecules, Plenum Press, New York, 1996, pp. 285–379.
[43] J. Kyte, R.F. Doolittle, J. Mol. Biol. 157 (1982) 105–132.